Available online at www.sciencedirect.com
SCIENCE DIRECT
Journal of Photochemistry and Photobiology A: Chemistry 174 (2005) 246–252
Journal of Photochemistry and Photobiology A:Chemistry
www.elsevier.com/locate/jphotochem

Global photonic efficiency for phenol degradation and mineralization in heterogeneous photocatalysis

Jorge Medina-Valtierra [a,c,*], Edgar Moctezuma [b], Manuel Sánchez-Cárdenas [a], Claudio Frausto-Reyes [c]

[a] *Departamento de Ingeniería Química y Bioquímica, Tecnológico de Aguascalientes, Av. Adolfo López Mateos No. 182 Ote., Fracc. Bona Gens, Aguascalientes, Ags. 20256, Mexico*
[b] *Escuela de Ciencias Químicas, Universidad Autónoma de San Luis Potosí, A. Obregón No. 64, San Luis Potosí, S.L.P. 78000, Mexico*
[c] *Centro de Investigaciones en Optica A.C., Unidad Aguascalientes, Prol. Constitución No. 607, Fracc. Reserva de Loma Bonita, Aguascalientes, Ags. 20200, Mexico*

Received 8 October 2004; received in revised form 24 March 2005; accepted 31 March 2005
Available online 21 April 2005

Abstract

Simple kinetic model is proposed for fitting experimental data of degradation and total organic carbon (mineralization) of phenol. Reaction rates analysis of phenol in water are employed to compare different photocatalysts under the same experimental conditions. The global photonic efficiency for degradation and mineralization of phenol ξ_g, is calculated to facilitate comparison with other photocatalysts or experimental systems. Under identical conditions of catalyst loading, pH and phenol concentration the most of photocatalysts presented a global efficiency much lower than that for a TiO_2 standard photocatalyst named Degussa P-25. However, two photocatalysts prepared by different methods showed approximately the same global efficiency than the commercial material.

Keywords: UV photocatalysis; Phenol photocatalytic mineralization; Titanium dioxide photocatalysts; Relative photonic efficiencies; Global photonic efficiency

1. Introduction

Photocatalytic oxidation offers an excellent possibility for removing variety of pollutants from contaminated waters. A number of advanced photooxidation technologies for water treatment, consisting of illumination by UV light of aqueous suspensions of TiO_2 exist.

Suitable treatments are ideally achieved in small-scale plants in order to prevent toxicity, which is easier to remove before transferring toxic materials to other medium.

However, highly efficient catalysts are still needed. Thus, development of new photocatalysts for pollution treatment is of current interest [1]. Nevertheless, from a range of semiconductor photosensitive materials, titanium dioxide is the most widely used photocatalyst due to its exceptional physical and chemical properties.

In some earlier papers [2–4] use of relative photonic efficiencies as a means of comparing photochemical processes has been described. These methods avoid knowing the amount of photons absorbed by the photocatalyst and attenuate other unidentified aspects by carrying the experiments under identical conditions. However, in other studies variations with respect to the absorbed photon flux were considered [5].

Some researchers recommend using formal rate constants in the photodegradation of organic substrates as a measure of the photo-oxidation efficiency [6]. However, when changes in the kinetic order occur, the use of rate constants is not recommendable. In such case it is preferable to base all measurements in the "rate of reaction".

* Corresponding author. Tel.: +52 449 9105002; fax: +52 449 9700423.
E-mail addresses: jormeval@yahoo.com (J. Medina-Valtierra), edgar@uaslp.mx (E. Moctezuma), msc@upa.com (M. Sánchez-Cárdenas), cfraus@cio.mx (C. Frausto-Reyes).

1010-6030/$ – see front matter © 2005 Elsevier B.V. All rights reserved.
doi:10.1016/j.jphotochem.2005.03.020

The present report extends the previous works to organic substrate disappearance and mineralization and proposes the applicability of a global efficiency measure since relative efficiencies of degradation or mineralization do not indicate which material is better than the other.

Here, it is reported on a method for the comparison of various photocatalysts into the same photocatalytic process. This is for determining the more efficient one for a given organic substrate by considering its transformation as well as its mineralization.

2. Experimental

2.1. Photocatalysts

Degussa P-25, with a composition anatase/rutile of 80/20, surface area of 55 $m^2\ g^{-1}$ and particle size of 30 nm was used as the reference photocatalyst without further treatment. The chemicals used in the experiments were of reagent grade and no additional purification was carried out. All solutions were prepared with deionized water.

To deposit thin films of TiO_2 on fiberglass two procedures described in literature for the deposition of anatase films on glass substrates were adopted: hydrolysis of TiF_4 [7] and dip-coating in a sol–gel solution [8].

A piece of 8 μm fiberglass purchased from Corning Inc. was used as the main substrate. Glass microscope slides were also used as substrates for reference samples. The substrates were cleaned for 2 h in an ultrasound bath with isopropanol, and then dried in an oven at 90 °C for 1 h.

In the first method, TiF_4 (Aldrich Chemical) was dissolved in deionized water to give a 0.04 M solution, then aqueous ammonia, NH_4OH (J.T. Baker) was added to 100 mL of this solution to adjust pH to 2. This solution was then heated to 70 °C and stirred for 1 h. Finally a portion of fiberglass and a glass side (75 mm × 25 mm × 2 mm) were immersed for 6 h into the solution maintained at 70 °C.

The preparation procedure of TiO_2 films by the sol–gel method is as follows: 2.97 mL of titanium (IV) isopropoxide (TIPO, 98%, Aldrich) were dissolved in 30 mL of ethanol (J.T. Baker) and stirred for 1 h. Then 0.8 mL of diluted HNO_3 (acid/water: 1/32 v/v, J.T. Baker) and 16 mL of ethanol were added to induce hydrolysis in the resulting solution. In some preparations cetyltrimethyl-ammonium bromide (CTAB, Aldrich) was added to the precursor solutions followed by 30 min stirring. In these cases the molar ratio TIPO/CTAB was adjusted between 4 and 16. The TiO_2 films were deposited on the fiberglass or on the glass substrates by dip-coating them in the sol–gel solution at ambient conditions.

TiO_2 film-loaded fiberglass was washed with deionized water at room temperature and then dried in electrical furnace at 110 °C for 1 h. After drying, samples were heated in static air at a rate of 5 °C min^{-1} up to the treatment temperature and held for 3 h. Finally the calcined fiber was ground using an agate mortar to obtain glass microrods with a macroscopic appearance of powder. In addition to the microrods coated with TiO_2 thin film, a powder TiO_2 sample was also obtained grinding the resulting solid after the drying and heating treatments. Thus, several different samples of TiO_2 were obtained by the two preparation processes: (1) a thin film deposited on the fiberglass by the hydrolysis method and without surfactant (FHM-NS); (2) thin films deposited on the fiberglass by the sol–gel technique without surfactant (FSG-NS); (3) thin films on the fiberglass by the sol–gel technique with surfactant (FSG-*n*), where *n* represents the number of moles of TIPO per mole of CTAB surfactant in the precursor sol–gel; and (4) powders by the sol–gel technique with or without surfactant, PSG-*n* or PSG-NS, respectively. The calcination temperatures of the materials are mentioned in Table 1.

2.2. Characterization techniques

Raman spectra of TiO_2 (primarily anatase form) from prepared samples were obtained with an instrumental set-up using a He–Ne laser (632.8 nm) and 10 mW of power at the sample (not presented here). Characteristic Raman peaks for anatase were determined by comparing their relative positions and intensities with the reported literature values [9]. A Visible Spectrophotometer Perkin-Elmer model Lambda 12 with a resolution of 0.1 nm was used to measure the optical transmittance spectra. TiO_2 films deposited on microscope slides were used to determine the range of UV absorption, while a Film Tek 3000 SCI system was coupled to the spectrophotometer to measure film thickness.

Table 1
Preparation and characterization data of the TiO_2 films and powders

Sample	Preparation procedure	Observation	Calcination temperature (°C)	TiO_2 loading (mg/g)	Film thickness (nm)	Surface area (m^2/g)
FHM-NS	Hydrolysis	No surfactant	400	3.41	75	–
FSG-NS	Sol–gel	No surfactant	450	2.87	61	–
FSG-16	Sol–gel	Surfactant	450	4.58	230	–
FSG-4	Sol–gel	Surfactant	450	4.21	538	–
PSG-NS	Sol–gel	No surfactant	500	–	–	<5
PSG-16	Sol–gel	Surfactant	500	–	–	5
PSG-8	Sol–gel	Surfactant	500	–	–	9
PSG-4	Sol–gel	Surfactant	500		–	54

The amount of TiO_2 deposited in the coated fiberglass was determined by atomic absorption spectrophotometry, AAS (Perkin Elmer Analyst 100) operating in the acetylene–N_2O flame mode. The titanium oxides' coating was dissolved by adding 0.1 g of the coated fiberglass to 10 mL of 50% chloridic acid in deionized water (v/v). This mixture was heated at 60 °C for 30 min to dissolve the TiO_2 completely. The final solution was cooled, filtered and transferred to a 50 mL volumetric flask and diluted to volume with deionized water.

The BET specific surface areas of the powder samples prepared through the same procedure as the thin films were determined using nitrogen adsorption measurements with an Accusorb 2100-E porosimeter. The BET specific surface areas of the TiO_2 thin films on the fiberglass could not be measured directly by the adsorption apparatus because the amount of the thin film on the substrate was too small.

2.3. Photoreactor and photocatalytic experiments

The experimental set-up used for the photocatalytic evaluation consisted of a batch reactor (100 mL volume) that was equipped with a blower to maintain a low temperature. Three 15 W mercury lamps (Cole-Parmer) placed equidistantly around the reactor were used as UV light source. The major peak of spectrum wavelength occurs at 365 nm, which is near to the absorption range for the anatase type of TiO_2 obtained in this study.

All experiments were carried out at pH 3.0 with 500 mg of a catalyst, suspended by magnetic stirring in the phenol solution. A preliminary test for the degradation kinetics of phenol without catalyst was also carried out.

Each experiment was performed at 30 °C with oxygen bubbling at a flow rate of 60 mL min^{-1}, when the phenol concentration was 40 mg L^{-1} (ppm), and 100 mL min^{-1} for a phenol concentration higher than 40 ppm. Small aliquots of the solution (2 μL) were periodically withdrawn to measure the concentration of phenol as a function of time. Phenol concentration was monitored by high performance liquid chromatography (HPLC) using a Waters 600E chromatograph equipped with an UV detector and a Novapak-Phenyl column. A 40:60 v/v mixture of methanol:(EDTA + monohydrated citric acid + water) at a flow of 0.7 mL min^{-1} was used as the eluent. Removal of total organic carbon (TOC) was measured by a Shimadzu TOC-5000A.

2.4. Phenol adsorption experiments

Adsorption of phenol on Degussa P-25 was determined by contacting the photocatalyst powder with a phenol solution for a given time in the photoreactor used also for photocatalytic experiments. Typically, the reactor was loaded with 100 mL of a phenolic solution of known concentration (100 mg L^{-1}), and different amounts of photocatalyst (ranging from 0 to 0.2 g). The stirring was then turned on, and regular liquid samples were taken in periods of 4 h and analyzed by HPLC.

3. Results and discussion

Dimensional and textural data of the samples (Table 1) show that the average thickness of the films was greater when they were prepared with surfactant than when they were prepared without surfactant. Additionally, the BET specific surface area of the TiO_2 powders prepared without surfactant was smaller than when they were prepared with surfactant. This is due to the removed surfactant from samples during heat treatment since when surfactant molecules are burned; they can leave pores into the material bulk.

3.1. Kinetics of phenol degradation and mineralization

First of all, amount of adsorbed phenol increases smoothly with increasing catalyst concentration. Phenol adsorption data obtained at 25 °C correlate the amount of phenol adsorbed per unit weight of catalyst where equilibrium concentration was reached in less than 2 h. When a catalyst loading of 2 g L^{-1} was used, phenol was adsorbed at a low value of 2 mg phenol/g of catalyst. Intermediates molecules formed during photodegradation of phenol could show an adsorptive behavior very different.

It has been found that the photoactivity and the photonic efficiency in the presence of Degussa P-25 and other photocatalysts depend on the catalyst loading. Although San et al. determined that the optimum concentration of TiO_2 for the degradation of 4-nitrophenol was 3 g L^{-1} [10], we used a photocatalyst loading of 5 g L^{-1} because it has been reported that the photonic efficiency can be lower for P-25 than for other photocatalytic materials above 2.5 g L^{-1} [5]. Moreover, the latter report showed that the dependence of photonic efficiency on the catalyst loading in the presence of Degussa P-25 showed an increasing until a photocatalyst concentration of 5 g L^{-1}.

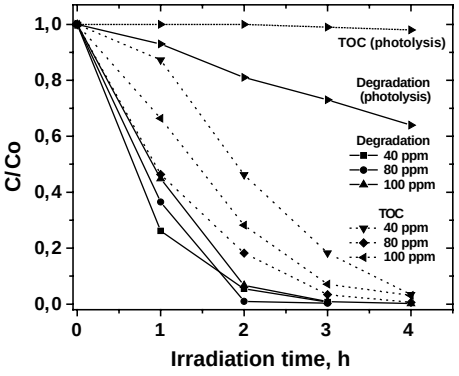

Fig. 1. Disappearance of phenol by photolysis, degradation (►, —) and mineralization (►, ···). Photocatalytic degradation and mineralization at different concentrations of phenol on TiO_2 powder (Degussa P-25).

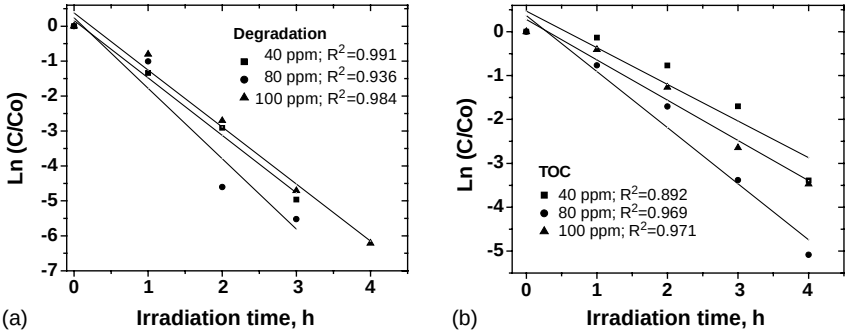

Fig. 2. Effect of initial conditions on the fit of first-order kinetics for the photodegradation (a) and mineralization (b) of phenol over Degussa P-25.

Fig. 1 shows the kinetics of the disappearance of phenol from an initial concentration of 100 mg L^{-1} under an UV irradiation and without any catalyst. In the absence of photocatalyst there was a measurable loss of phenol, ca. 36%, due to degradation. However, under the same conditions, the mineralization was not significant.

The degradation and mineralization to total organic carbon (TOC) for three different concentrations of phenol in the presence of the commercial P-25 TiO_2 are also shown in Fig. 1. In all cases, a rapid degradation of phenol occurred and the phenol concentration decreased less than 5% after irradiation for 2–3 h. It can be seen that the mineralization of phenol in the presence of TiO_2 P-25 showed a lower yield. This is understandable because the mineralization process involves several steps before total removal of all organic intermediates is achieved. Nevertheless, photomineralization higher than 94% was reached after 4 h of irradiation.

The evolution of curves is according to apparent first-order kinetics, $\ln(C/C_0) = kt$, where C_0 is the initial concentration and C the concentration of phenol at time t. Hence, the logarithm plots of C/C_0 data gave straight lines as shown in Fig. 2.

The correlation constants (R^2) for the fitted lines were calculated to be between 0.99 and 0.89. R^2 values of 0.99, 0.98 and 0.94 for degradation data indicate that the photocatalytic degradation of phenol can be described by the first-order kinetic model. The results of TOC degradation analysis, shown in Fig. 2 indicate that at lower levels of TOC degradation, according to the low value for R^2 of 0.892, reactions appeared

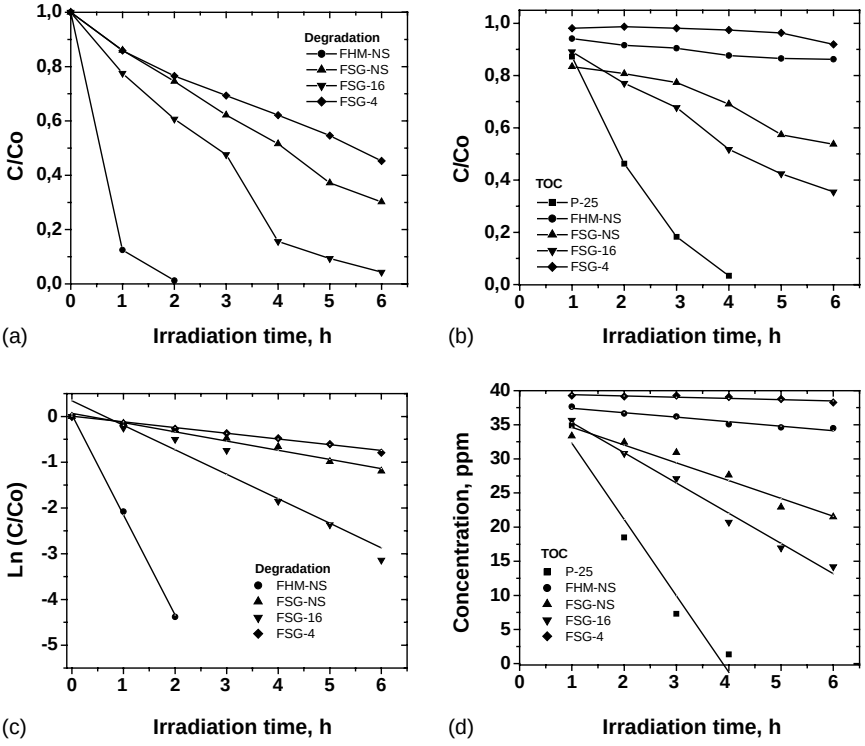

Fig. 3. Photocatalytic degradation (a) and mineralization (b) of phenol over deposited TiO_2 thin films. Reaction rate kinetics for degradation (c) and mineralization (d) of phenol. TOC and the dependence of the concentration of phenol on the irradiation-time over Degussa P-25 (■) was added.

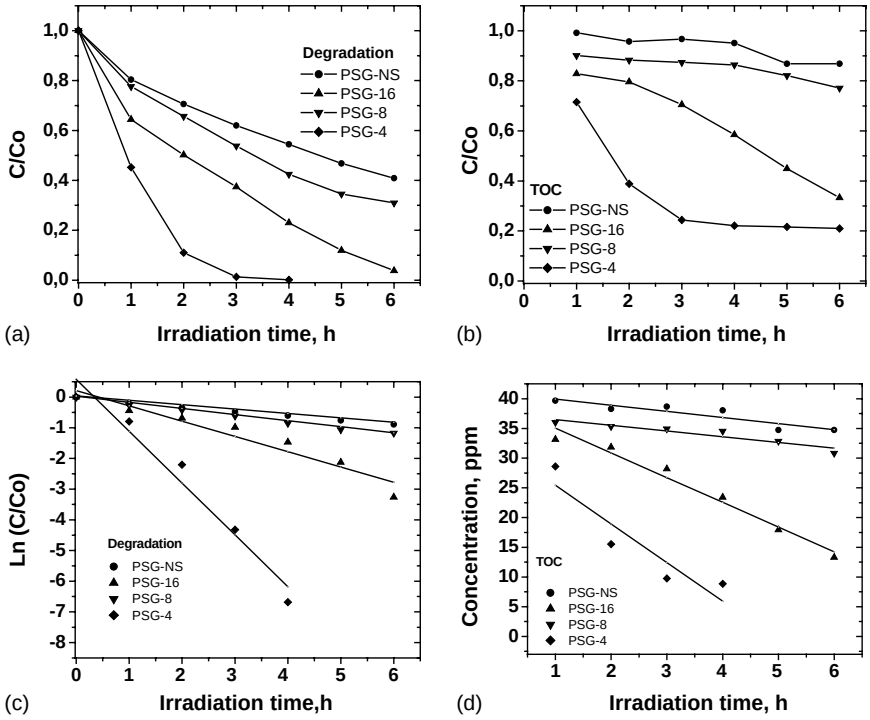

Fig. 4. Photocatalytic degradation (a) and mineralization (b) of phenol over different TiO_2 powders. Reaction rate kinetics for degradation (c) and mineralization (d) of phenol.

to follow a simple model like zero-order kinetics. To avoid overlaps between first and zero order kinetics, in following experiments an initial phenol concentration of 40 mg L^{-1} and an oxygen flow rate of 60 mL min^{-1} were used. At these conditions it is expected that mineralization data fit to zero-order kinetics.

3.2. Relative photonic efficiencies for phenol degradation and mineralization

Plots of normalized concentration vs. irradiation-time for eight different photocatalysts (FHM, FSG and PSG samples) are reported in Figs. 3 and 4. Again, the rates of the photocatalytic degradation could be fitted to simple first-order kinetics.

Fig. 1 showed TOC conversion as a function of time in the presence of the commercial TiO_2 using the same amount of photocatalyst but varying the phenol concentration. In all next experiments, the same TOC of phenol was calculated as the initial concentration (∼33 ppm). Unfortunately, this value was not measured with precision a time zero, because phenol adheres to the reactor walls and to the fiberglass microrods due to the hydrophobicity in this aqueous system. As a consequence, initial TOC measured was usually low at the beginning of treatment, but reached a normal value after this induction period (<1 h). From TOC curves it is possible to see that mineralization, once begun, maintains the same slope at exception for the PSG-4 photocatalyst. This means that is possible to fit directly a zero-order kinetics: $C - C_0 = kt$. To evaluate results from PSG-4 sample only the first four points were considered. Alternatively, a first-order fit could be done if all points are took account.

The experimental results shown in Figs. 3 and 4 have been used to calculate the rate constants for degradation reaction (k_1) and mineralization reaction (k_0). By using kinetic expressions these constants can be calculated from the slope of the lines of fit, which are shown in the same figures.

The experimental results agree reasonably well with the model proposed and the constants were determined from experimental data. Thus, initial rates were calculated using these rate constants (Tables 2 and 3).

Photodegradation initial rates of phenol were calculated from the equation: $r_0 = k_1 C_0$, for an apparent first-order kinetics when the phenol concentration C_0 is small [10]. Initial rates of mineralization of phenol were calculated from: $r_0 = k_0$, for an apparent zero-order kinetics. In this case, ap-

Table 2
Predicted values of rate constants and initial reaction rates for the first-order kinetics in the photodegradation of phenol

Sample	k_1 (h^{-1})	R^2	r_0 (ppm h^{-1})
P-25	1.643	0.991	65.72
FHM-NS	2.191	0.997	87.64
FSG-NS	0.201	0.981	8.04
FSG-16	0.536	0.939	21.43
FSG-4	0.1214	0.991	4.99
PSG-NS	0.144	0.994	5.760
PSG-16	0.498	0.929	19.92
PSG-8	0.199	0.994	7.96
PSG-4	1.689	0.964	67.56

Table 3
Predicted values of rate constants and initial reaction rates for the zero-order kinetics in the photomineralization of phenol

Sample	k_0 (ppm h^{-1})	R^2	r_0 (ppm h^{-1})
P-25	11.187	0.958	11.19
FHM-NS	0.657	0.950	0.66
FSG-NS	2.606	0.967	2.61
FSG-16	4.430	0.989	4.43
FSG-4	0.183	0.769	0.18
PSG-NS	0.967	0.835	0.97
PSG-16	4.160	0.973	4.16
PSG-8	1.030	0.889	1.03
PSG-4	6.503	0.85	6.50

Table 4
Relative and global photonic efficiencies for the different photocatalytic samples with Degussa P-25 TiO_2 as the standard reference

Sample	ξ_d	ξ_m	ξ_g
P-25	1.000	1.000	1.000
FHM-NS	1.333	0.059	0.950
FSG-NS	0.122	0.233	0.435
FSG-16	0.326	0.396	0.578
FSG-4	0.076	0.016	0.256
PSG-NS	0.087	0.086	0.349
PSG-16	0.303	0.372	0.562
PSG-8	0.121	0.092	0.371
PSG-4	1.028	0.581	0.962

propriate conditions were used to have a probable saturation of the surface of TiO_2 with adsorbed molecules (phenol and intermediates) in order not to affect the reaction rates by initial concentration of phenol [4].

As seen from straight lines of Figs. 3 and 4 and R^2 values in Table 3, fits for mineralization are not perfect, but taking into account the experimental and accumulative errors, the adjustment may be considered acceptable.

3.3. Global photonic efficiency for phenol degradation and mineralization

The concept of relative photonic efficiency ξ_d, introduced by Tahiri et al. [2], has been used because it is a useful tool that renders comparison of process efficiencies with different organic substrates. Nevertheless, instead of different substrates different photocatalyst samples were used. This is also a relative efficiency relating degradation rates,

$$\xi_d = \frac{\text{rate of phenol disappearance on Degussa P-25}}{\text{rate of phenol disappearance on the photocatalyst}} \quad (1)$$

Other concept of relative photonic efficiency that relates mineralization instead of initial degradation rate introduced by Malato et al. [4], has been adapted to complement the comparison of process efficiencies with different photocatalysts,

$$\xi_m = \frac{\text{rate of phenol mineralization on Degussa P-25}}{\text{rate of phenol mineralization on the photocatalyst}} \quad (2)$$

Phenol (40 mg L^{-1}) has been used to calculate ξ_d and ξ_m in order to follow the method proposed by the above-mentioned authors.

In this work, a global photonic efficiency parameter was used to follow the rates of disappearance and TOC degradation of phenol due to the fact that both processes are very important and complementary. Thus we propose,

$$\xi_g = \frac{\xi_d + (\xi_m)^{1/5}}{2} \quad (3)$$

where ξ_d and ξ_m are obtained with Eqs. (1) and (2).

As can be noted, the above equation is a very simple expression, however, if the transformation of intermediates detected or the direct coupling of two phenoxy radicals are regarded, then this can be lead to a more complex kinetic expression.

The equation proposed above is supported by a general mechanism of the photocatalytic degradation of phenol. As proposed by several authors, all oxidation routes consider the hydroxylation of phenol to hydroquinone and catechol as a first step [10–13]. These detected intermediates can be rationalized assuming the existence of an activation of the phenol molecule by reaction with an $OH^\bullet$ radical. Further oxidation of the dihydroxybenzenes gives benzoquinones.

A complete mineralization to CO_2 as a final product involves breaking of C–C bonds and decarboxylation of intermediates such as maleic, acetic, oxalic or formic acid by further reaction with $OH^\bullet$ radicals. Each bond breaking is accompanied by the formation of an acid with shorter chain and a CO_2 molecule. For example, mucinic acid is obtained from the first breakage of the benzoquinone [13], while decarboxylation of mucinic acid gives maleic acid.

In addition, all intermediates can suffer an attack with $OH^\bullet$ radicals in a way similar to phenol. Therefore, if we only consider the breakage of C–C bonds, the disappearance (degradation) of the aromatic ring (phenol) happens when the first C–C bond is broken. For a complete mineralization (TOC) six C–C bonds have to be broken.

The value of ξ_g means the average between the degradation of phenol detected from the first C–C bond broken and the TOC expected from intermediates that suffered the breakage of five C–C bonds.

Using Eqs. (1)–(3), relative and global photonic efficiencies of the different photocatalysts were calculated and after reported in Table 4.

All the global efficiencies are lower than one, indicating that the maximum photocatalytic oxidative degradation of the photocatalytic samples at the selected initial concentration was obtained with Degussa P-25, although two samples give values for ξ_g close to 1.

Consequently, it can be concluded that in comparison to the Degussa P-25, only two TiO_2 photocatalysts synthesized in this work as thin film and powder (FHM-NS and PSG-4), exhibit a nearly comparative global activity for the degradation of phenol and oxidation of phenol intermediates to CO_2.

4. Conclusions

Satisfactory agreement between the experimental and predicted concentration–time profiles for degradation and TOC was demonstrated.

Global photonic efficiency based on the initial rates of degradation illustrates all aspects of photodegradation of organic contaminants for water treatment purposes.

The use of global photonic efficiency ξ_g, instead of relative photonic efficiencies renders a total comparison of process efficiencies (relative to phenol at the same initial conditions as contaminant concentration, catalyst loading, temperature and pH in the photoreactor). These global photonic efficiencies can be used to compare photonic efficiencies of distinct photocatalyst materials and thus to determine which one can transform more efficiently phenol as probe molecule. Other types of catalysts as well as organic substrates could be probed.

Acknowledgements

The authors wish to thank Miss Jitka Kirchnerova, École Polytechnique de Montréal, for her assistance in the revision of the final manuscript. Financial support from CIO, AC, Project No. 203TM-012, is acknowledged.

References

[1] J.C. Yu, W. Ho, J. Yu, S.K. Hark, K. Lu, Langmuir 19 (2003) 3889–3896.
[2] H. Tahiri, N. Serpone, R.L. van Mao, J. Photochem. Photobiol. A: Chem. 93 (1996) 199–203.
[3] N. Serpone, G. Sauvé, R. Koch, H. Tahiri, P. Pichat, P. Piccinini, E. Pelizzetti, H. Hidaka, J. Photochem. Photobiol. A: Chem. 94 (1996) 191–203.
[4] S. Malato, J. Blanco, C. Richter, M.I. Maldonado, Appl. Catal. B: Environ. 25 (2000) 31–38.
[5] C. Wang, J. Rabani, D.W. Bahnemann, J.K. Dohrmann, J. Photochem. Photobiol. A: Chem. 148 (2002) 169–176.
[6] F. Sabin, T. Turk, A. Vogler, J. Photochem. Photobiol. A: Chem. 63 (1992) 99–106.
[7] K. Shimizu, H. Imai, H. Hirashima, K. Tsukuma, Thin Solid Films 351 (1999) 220–224.
[8] Ch. Wu, L. Tzeng, Y. Kuo, Ch.H. Shu, Appl. Catal. A: Gen. 226 (2002) 199–211.
[9] J. Yu, X. Zhao, Q. Zhao, Thin Solid Films 379 (2000) 7–14.
[10] N. San, A. Hatipoglu, G. Kocturk, Z. Cinar, J. Photochem. Photobiol. A: Chem. 146 (2002) 189–197.
[11] L.J. Alemany, M.A. Bañares, E. Pardo, F. Martin, M. Galán-Fereres, J.M. Blasco, Appl. Catal. B: Environ. 13 (1997) 289–297.
[12] A.M. Peiró, J.A. Ayllón, J. Peral, X. Doménech, Appl. Catal. B: Environ. 30 (2001) 359–373.
[13] A. Santos, P. Yustos, S. Rodríguez, F. García-Ochoa, Appl. Catal. B: Environ. 39 (2002) 97–113.